Available online at www.sciencedirect.com
ScienceDirect
Carbohydrate Polymers 69 (2007) 799–804
Carbohydrate Polymers
www.elsevier.com/locate/carbpol

Short communication

Imaging cellulose fibre interfaces with fluorescence microscopy and resonance energy transfer

Cameron I. Thomson [a], Robert M. Lowe [b], Arthur J. Ragauskas [a,*]

[a] School of Chemistry and Biochemistry, Georgia Institute of Technology, Atlanta, GA 30332-0400, USA
[b] School of Chemical and Biomolecular Engineering, Georgia Institute of Technology, Atlanta, GA 30332-0400, USA

Received 13 December 2006; received in revised form 27 January 2007; accepted 29 January 2007
Available online 9 February 2007

Abstract

Future developments in cellulosic materials are predicated by the need to understand the fundamental interactions that occur at cellulose fibre interfaces. These interfaces strongly influence the material properties of fibre networks and fibre reinforced composites. This study takes advantage of fluorescence resonance energy transfer (FRET) and fluorescence microscopy to image cellulose interfaces. Steady-state epi-fluorescence microscopy suggests that energy transfer from coumarin dyed fibres to fluorescein dyed fibres is occurring at the fibre–fibre interface. The FRET response for natural spruce fibre interfaces is distinctly different from that observed in synthetic viscose fibres. This approach constitutes a novel methodology for the characterization of soft material interfaces on the molecular scale, and represents a major opportunity for advancing the understanding of fibrous network structures.
© 2007 Elsevier Ltd. All rights reserved.

Keywords: Cellulose fibres; Fibre bonding; Fluorescence resonance energy transfer; Fluorescence microscopy

1. Introduction

The development of biomass-derived materials is receiving increased focus primarily due to the need for sustainable green chemistry processes and materials (Bridgwater, 2003; Council, 2000; Ragauskas et al., 2006). Cellulose fibres are particularly attractive for incorporation into advanced materials due to their ubiquitous renewable production, facile isolation and strength properties. Cellulose fibres have been extensively investigated for potentially unique applications in composites (Gindl, Schoeberl, & Keckes, 2006; Zadorecki, Karnerfors, & Lindenfors, 1986), nanocomposites (Berglund, 2005; Choi & Simonsen, 2006), and as scaffolds in tissue engineering (Eichhorn et al., 2006). A fundamental understanding of fibre–fibre interfaces is critical to the design and fabrication of networked structures such as composites because stress transfer between load bearing fibres operates through fibre–fibre and fibre–matrix interfaces. For composites with high fibre/matrix volume ratios, the percentage of fibre specific surface area (m^2/kg) that is close enough to facilitate molecular interactions such as hydrogen bonding or attractive van der Waals forces (Notley, Pettersson, & Wagberg, 2004) is of critical importance to their physical performance properties (Lindstrom, Wagberg, & Larsson, 2005). Fibre–fibre interfaces are also important to composites with low fibre/matrix volume ratios. For example, Dufresne and Favier et al. have concluded that the formation of a network of tunicin cellulose whiskers is responsible for the dramatic increase in Young's modulus of composites containing just 5% cellulose whiskers, by volume (Dufresne, 2003; Favier, Canova, Shrivastava, & Cavaille, 1997). Despite the importance of fibre–fibre interfaces to both nano- and macro-scale network structures the need for proper characterization has not been fully addressed.

This study is directed to provide a new approach for characterizing fibre-fibre distance constraints at the interface. Our approach is to functionalize a cellulose fibre

* Corresponding author. Tel.: +1 404 894 9701; fax: +1 404 894 4778.
E-mail address: arthur.ragauskas@chemistry.gatech.edu (A.J. Ragauskas).

0144-8617/$ - see front matter © 2007 Elsevier Ltd. All rights reserved.
doi:10.1016/j.carbpol.2007.01.023

system with a pair of fluorescent dyes capable of fluorescence resonance energy transfer (FRET) and then utilize fluorescence microscopy to provide images of relative energy transfer values within fibre–fibre interfaces. These relative energy transfer values are proportional to the distances between labelled fibre surface components that comprise the fibre–fibre interface.

Forster developed a theory for the long range radiationless transfer of energy between chromophores almost sixty years ago (Forster, 1948), now commonly referred to as FRET. FRET occurs when two fluorophores within 1–10 nm have sufficient quantum yields, favourable dipole–dipole orientations, and significant spectral overlap between the donor emission and acceptor absorption spectra (Van Der Meer, Coker, III, & Chen, 1994). The phenomenon has been used as a powerful tool in biochemistry for the measurement of molecular distances with applications to the investigation of protein dynamics (Somogyi et al., 1984) and sensing strategies (Takakusa et al., 2002). Wong and Groves (Wong & Groves, 2001; Wong & Groves, 2002) studied an analogous system to that of fibre crossings while imaging the topography of lipid bilayers via intermembrane resonance energy transfer.

2. Experimental

2.1. Materials

Viscose staple fibre was acquired from Lenzing AG (Austria). The fibres were 1.2 denier (1.2 g/9000 m length), manually cut to an average length of 1.9 mm, washed thoroughly with deionized water and air-dried prior to dyeing. The spruce fibre is a never dried bleached white spruce (*Picea glauca*) kraft pulp obtained from Alberta Pacific (Canada). The pulp was lab bleached with chlorine dioxide and fully washed prior to dyeing. The fibre properties were determined using an OpTest Fibre Quality Analyzer. The average fibre length is 2.5–3.0 mm; the fibre width is 25–75 μm and the cell wall thickness is 1–3 μm. 7-Diethylaminocoumarin-3-carboxylic acid hydrazide (DCCH) and fluorescein-5-thiosemicarbazide (FTSC) were obtained from Molecular Probes (Eugene, OR, USA) and used as received. All other chemicals were obtained from Aldrich and used as received.

2.2. Instrumentation

Steady state epi-fluorescence micrographs were collected under controlled temperature and humidity (50% relative humidity and 23 °C) using a Leica inverted light microscope equipped with a fluorescence disc for fast changes between filter sets. Custom filter cubes were manufactured by Chroma Technology Corp (Rockingham, VT). The filter sets are chosen to separate three distinct signals (EX/EM): the donor fluorescence (440 nm/480 nm); the directly excited acceptor fluorescence (500 nm/525 nm long pass); and the acceptor fluorescence due to FRET (440 nm/525 nm long pass). Digital images were collected using a Hamamatsu ORCA-ER digital camera.

Fluorescence spectra were collected under ambient conditions using an ISS PC-1 steady-state fluorescence spectrophotometer equipped with a 300 W xenon arc lamp and a R928 PMT (Hamamatsu) photon-counting detector. The excitation and emission monochromator slits were set to achieve 8 and 4 nm spectral bandwidths, respectively, and the front-face sample holder was set to an angle of 22.5°. Spectra were collected using a step size of 1 nm and a 1 s integration time.

2.3. Functionalizing fibres with fluorescent dyes

The model system in this study consists of natural and regenerated cellulose fibres labelled with a fluorescein/coumarin dye pair via covalent hydrazone linkages as shown in Fig. 1.

Both fluorescent dyes, DCCH (donor) and FTSC (acceptor) are commercially available from Molecular Probes (Eugene, OR) and have been used for various FRET applications (Van Der Meer et al., 1994; Mitsui, Nakano, & Yamana, 2000; Czworkowski, Odom, & Hardesty, 1991). The dyes were applied to the fibres using a method adapted from Anderson (Anderson, 1986). Fibre suspensions (3% w/w) were dyed overnight in glass vials containing either 1.6 mmol/L solution of FTSC in 15 mL dimethylformamide or 1.6 mmol/L solution of DCCH in 15 mL methanol. Both systems contained 28 μmol of HCl to catalyze the reaction. After dyeing, the fibres were briefly washed with DMF (50 mL) and then subjected to a mild sodium borohydride (0.50 g fibre and 0.02 mmol $NaBH_4$) treatment in DMF (15 mL) for 1 h. The fibres were again washed with DMF (50 mL), placed in cellulose extraction thimbles, then Soxhlet extracted with acetonitrile overnight to remove any excess dye. Precautions were taken throughout the process to minimize sample exposure to light. Prior

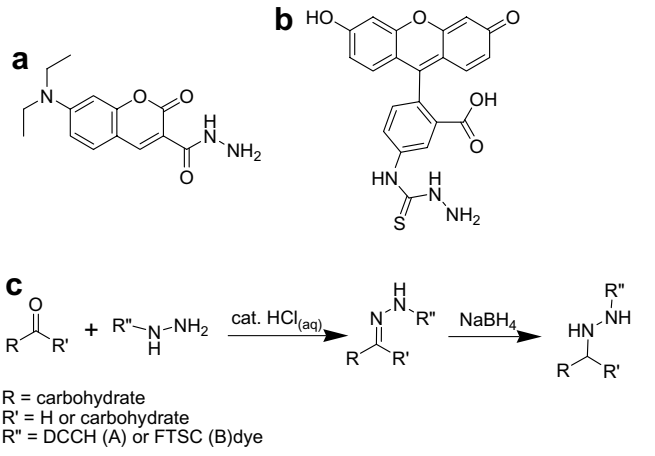

Fig. 1. (a) Structure of donor, 7-diethylaminocoumarin-3-carboxylic acid hydrazide (DCCH); (b) structure of acceptor, fluorescein-5-thiosemicarbazide (FTSC); (c) schematic of dyeing chemistry adapted from Anderson (Anderson, 1986).

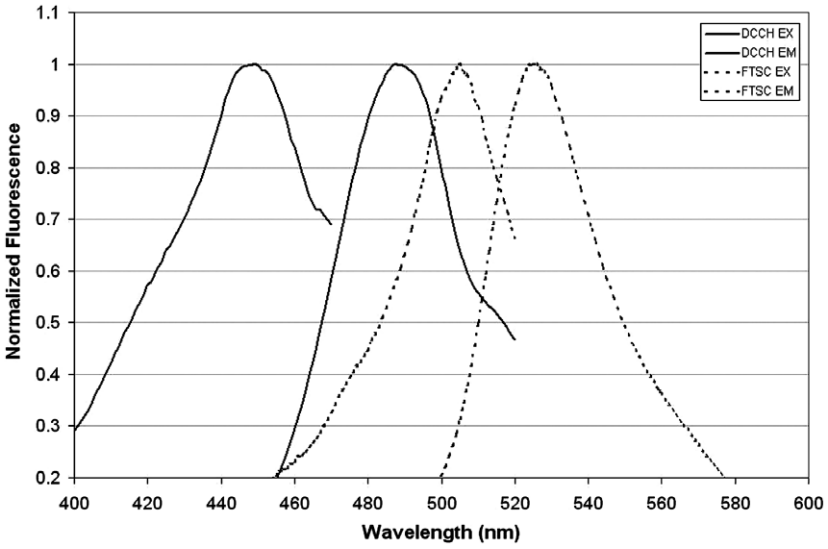

Fig. 2. Excitation and emission spectra of DCCH (—) and FTSC (---) dyed viscose fibre.

to microscopy, small sheets of viscose fibre were prepared in order to determine the excitation and emission fluorescence spectra of the dyes covalently linked to cellulose by steady state front face fluorescence spectroscopy. The spectra of the DCCH and FTSC dyed viscose fibres are shown in Fig. 2.

2.4. Fibre crossing preparation

Dilute suspensions (50 mg/L) of mixed fluorescein-dyed and coumarin-dyed fibres were prepared in deionized water and adjusted to pH 9 with 0.005 mol/L sodium tetraborate decahydrate buffer. Fibre intersections, as shown in Fig. 3, were prepared on glass slides by first filtering the suspension onto filter paper. The fibres were then transferred to glass slides with light pressing followed by air-drying at 50% relative humidity and 23 °C in a controlled temperature and humidity room for at least 6 h.

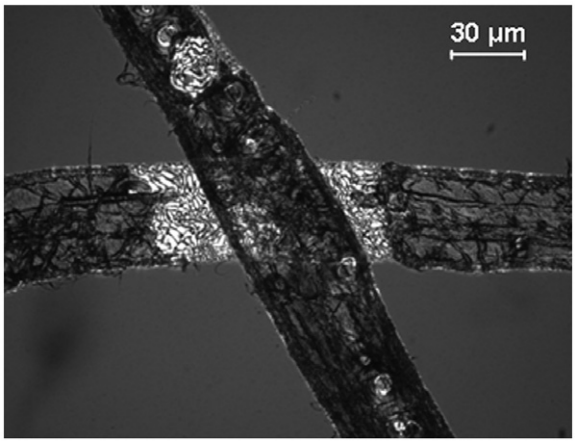

Fig. 3. Representative reflected light micrograph of a wood fibre crossing on a glass slide. Magnification 600×.

2.5. Image analysis

The measurement of FRET can be complicated by local dye concentration changes and inefficiencies in the microscope filter sets. The recent FRETN algorithm developed by Gordon (Gordon, Berry, Liang, Levine, & Herman, 1998) was employed in this work to correct the signal at each pixel. Twenty crossings were analyzed for each condition and each fibre crossing was analyzed by the collection of three fluorescence micrographs using three different filter sets. The FRETN correction method described below requires values for samples containing exclusively donor or acceptor dye. That requirement is met by obtaining average gray scale intensities from non-crossing regions on each of the fibres using three filter sets. Donor only, acceptor only, and both donor and acceptor conditions are measured with each of the three filter sets giving a total of nine values for the analysis. These nine values are then used to calculate the corrected FRETN value at each pixel in the crossing using MATLAB and the MATLAB Image Analysis Toolpak. Eqs. (1)–(5) are adapted from Gordon et al. and used to calculate FRETN for fibre crossings. The first (capitalized) letter in each term refers to the Filter set employed – FRET, Donor, or Acceptor. The second letter refers to the section of the picture where the value was collected: the acceptor fibre,"a;" the donor fibre, "d;" or the fibre crossing, "x;" For example, "Dx" refers to the signal from the fibre crossing using the donor filter set in the microscope.

$$\overline{\mathrm{Axa}} = \frac{\mathrm{Ax} - (\mathrm{Ad}/\mathrm{Fd})\mathrm{Fx}}{1 - (\mathrm{Fa}/\mathrm{Aa})(\mathrm{Ad}/\mathrm{Fd})} \tag{1}$$

$$\mathrm{FRET1} = \frac{\mathrm{Fx} - (\mathrm{Fa}/\mathrm{Aa})\mathrm{Dx} - \overline{\mathrm{Axa}}[(\mathrm{Fa}/\mathrm{Aa}) - (\mathrm{Fd}/\mathrm{Dd})(\mathrm{Da}/\mathrm{Aa})]}{G[1 - (\mathrm{Da}/\mathrm{Fa})(\mathrm{Fd}/\mathrm{Dd})]} \tag{2}$$

$$\overline{\mathrm{Dxd}} = \mathrm{Df} + \mathrm{FRET1}[1 - G(\mathrm{Da}/\mathrm{Aa})] - \overline{\mathrm{Axa}}(\mathrm{Da}/\mathrm{Aa}) \quad (3)$$

$$\mathrm{FRETN} = \frac{\mathrm{FRET1}}{\overline{\mathrm{Dxd}} \cdot \overline{\mathrm{Afa}}} \quad (4)$$

$$G = \frac{\mathrm{QY_A}}{\mathrm{QY_D}} \frac{\phi_\mathrm{A}}{\phi_\mathrm{D}} \frac{T_\mathrm{F}}{T_\mathrm{D}} \quad (5)$$

Eq. 5 is a factor relating the donor emission decrease as measured by the donor filter set to the acceptor emission increase measured by the acceptor filter set where $\mathrm{QY_A}$ and $\mathrm{QY_D}$ are the quantum yields of the two dyes. Φ_A refers to the fraction of acceptor fluorescence transmitted by the acceptor cube. Φ_D is the fraction for the donor fluorescence transmitted by the donor cube. T_F and T_D are the percent transmissions of the neutral density filters in the FRET and Donor filter sets, respectively. Literature values were used for the quantum yields and the other factors were obtained from the filter set spectra given to us by Chroma Technology.

The projected crossing area is calculated planimetrically in MatLab from each fibre crossing in the reflected light image. This normalization for crossing area is necessary in order to account for the inherent variation in the dimensions of the natural fibres and to provide a basis for the comparison of the two fibre sources.

3. Results and discussion

The primary region of interest in Fig. 3 is the fibre crossing area where both donor and acceptor dyes are present and FRET can occur. Fig. 4a shows the representative FRETN surface plot from a viscose fibre crossing.

Striations on the viscose fibres manifest themselves as a 'waffle like' pattern in the FRETN surface. It stands to reason that this type of response is the result of the high ridges on each fibre contacting each other. There are no regions in the viscose fibre interface with high levels of energy transfer. Fig. 4b shows the FRETN surfaces for crossings consisting of natural wood (*Picea glauca*) fibres. This interface is significantly different from that of the more regular viscose fibres and demonstrates areas of closer contact as shown by the color coded FRETN legend. Fig. 5 compares the pixel distributions of spruce and viscose fibre intersections.

This histogram is composed of all FRETN pixels for all crossings in each condition and is normalized for the total projected crossing area of those crossings. The viscose crossings have a tight distribution of pixels with low FRETN values, while the spruce fibres have a more broad distribution with a greater population of pixels with high FRETN values.

These results suggest that spruce pulp fibres will have a higher degree of bonding than viscose fibres. This result is supported by measurements of the ultimate strength of individual fibre–fibre joints in the literature. McIntosh and Leopold observed that fibre–fibre bonds were nearly seven times stronger than fibre–cellophane bonds (McIntosh & Leopold, 1961). Likewise, it has been observed that untreated rayon fibres (Mohlin, 1975; Torgnysdotter & Wagberg, 2003) demonstrate lower joint strengths as compared to wood fibers. There is evidence that natural fibres have several advantages over viscose fibres that can lead to superior performance in cellulose fibre composites (Eichhorn et al., 2001; Borja, Riess, & Lederer, 2006). However, the advantages of natural fibers are not limited to fibre–fibre bonding and thus the findings from this study may not fully explain the benefits of natural fibres incorporated into cellulose reinforced composites.

Recent observations of the surfaces of natural wood fibres in the wet state with atomic force microscopy indicate that these surfaces are highly fibrillar in nature (Furuta & Gray, 1998; Hanley & Gray, 1999; Pang & Gray, 1998). Several researchers have also observed that these fibrils are extended in solution (Pang & Gray, 1998; Chhabra, Spelt, Yip, & Kortschot, 2005). Furthermore, microindentation methods have indicated that natural wood fibre surfaces are highly compliant to depths of 200–800 nm into the cell wall (Chhabra et al., 2005). Unlike regenerated cellulose,

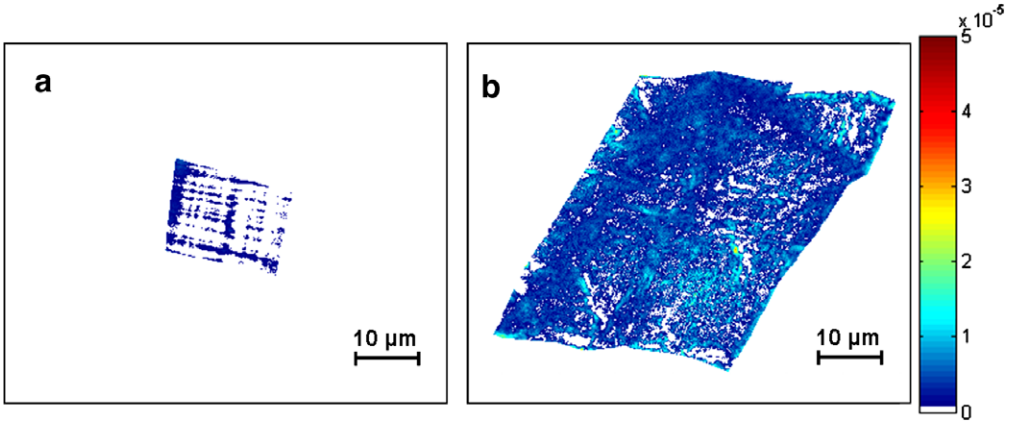

Fig. 4. Representative FRETN surface plots of (a) viscose fibre crossing and (b) wood fibre crossing on glass. The units for the colour coded legend are $\times 10^{-5}$ FRETN arbitrary units.

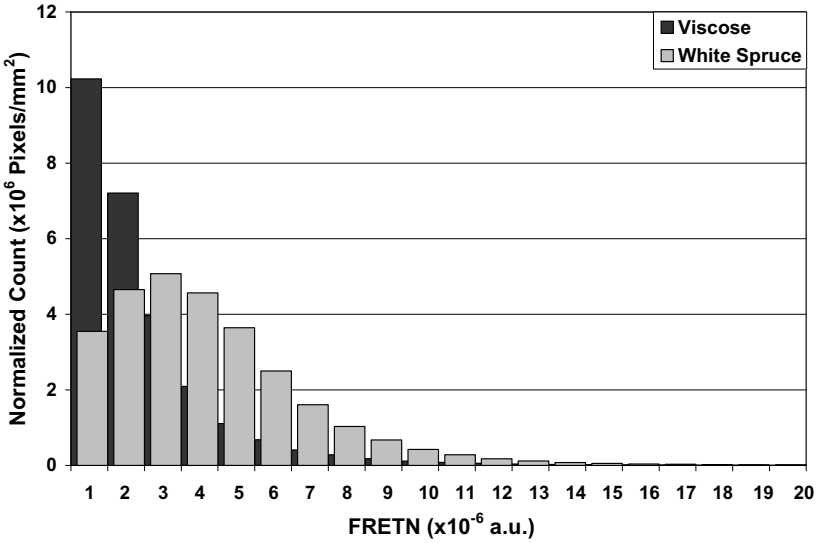

Fig. 5. Cumulative FRETN image histograms for comparison of viscose and spruce fibre crossings.

the surfaces of wood fibres contain amorphous low molecular weight polysaccharides (Hartler & Mohlin, 1975) which may be capable of interdiffusion thus leading to adhesion at the fibre–fibre bond (McKenzie, 1984). These low molecular weight components have lower glass transition points than pure cellulose and are likely to deform considerably under ambient conditions (Goring, 1965). The viscose fibres used in this study had smooth ridges running parallel to the fibre axis that were not amenable to the formation of large areas of intimate fibre–fibre contact. The results obtained in this study reflect the differences in surface morphology and topochemistry for natural and regenerated cellulose fibres.

Furthermore, a FRET response due to interdiffusion has been observed by Winnik et al. for the coalescence and film formation of various latex particles in nonaqueous dispersions (Pekcan, Winnik, & Croucher, 1990; Pekcan, Egan, Winnik, & Croucher, 1990; Oh et al., 2003; Wu, Tomba, Winnik, Farwaha, & Rademacher, 2004). Although their studies did not include imaging, the latex systems studied bear an analogy to the cellulosic fibre interfaces in this work. Thus, the entanglement of compliant fibrils combined with the intermixing of lower molecular weight polysaccharides is likely responsible for the increased areas of closer contact for wood fibres as measured by FRETN. It may be possible to combine both approaches which would provide dynamic topographical information as well as mechanistic and kinetic details of cellulosic interface development using FRET.

4. Conclusions

For the first time, cellulose fibre interfaces can be imaged using FRET and fluorescence microscopy. Steady-state epi-fluorescence microscopy suggests that energy transfer from coumarin dyed fibers to fluorescein dyed fibres is occurring. This is also the first known observation of nonradiative energy transfer occurring between objects of this scale. The FRET response for spruce fibre interfaces is distinctly different from that observed in viscose fibre. The fibrillar structure of spruce fibre surfaces and the presence of low molecular weight hemicelluloses is likely responsible for this difference. We anticipate that this methodology will allow the research community to make a significant contribution to the understanding of carbohydrate interfaces in a variety of advanced materials including, but not limited to, fibrous systems.

Acknowledgements

The authors thank Delphine Nain for her assistance with image processing in MatLab. C.I.T. acknowledges helpful discussions with Lauri Lehtonen. The authors also thank the Member companies of the Institute of Paper Science and Technology and the IPST@GT fellowship program for financial support. Portions of this work were used by C.I.T. and R.M.L. as partial fulfillment of the requirements for the Ph.D. degree at the Georgia Institute of Technology.

References

Anderson, J. M. (1986). Fluorescent hydrazides for the high-performance liquid chromatographic determination of biological carbonyls. *Analytical Biochemistry, 152*, 146–153.

Berglund, L. (2005). Cellulose-based nanocomposites. *Natural Fibers, Biopolymers, and Biocomposites*, 807–832.

Borja, Y., Riess, G., & Lederer, K. (2006). Synthesis and characterization of polypropylene reinforced with cellulose I and II fibers. *Journal of Applied Polymer Science, 101*, 364–369.

Bridgwater, A. V. (2003). Renewable fuels and chemicals by thermal processing of biomass. *Chemical Engineering Journal (Amsterdam, Netherlands), 91*, 87–102.

Chhabra, N., Spelt, J. K., Yip, C. M., & Kortschot, M. T. (2005). An investigation of pulp fiber surfaces by atomic force microscopy. *Journal of Pulp and Paper Science, 31*, 52–56.

Choi, Y., & Simonsen, J. (2006). Cellulose nanocrystal-filled carboxymethyl cellulose nanocomposites. *Journal of Nanoscience and Nanotechnology, 6*, 633–639.

National Research Council (2000). Biobased industrial products: priorities for research and commercialization. National Academy Press: p. 147.

Czworkowski, J., Odom, O. W., & Hardesty, B. (1991). Fluorescence study of the topology of messenger RNA bound to the 30S ribosomal subunit of *Escherichia coli*. *Biochemistry, 30*, 4821–4830.

Dufresne, A. (2003). Interfacial phenomena in nanocomposites based on polysaccharide nanocrystals. *Composite Interfaces, 10*, 369–387.

Eichhorn, S. J., Baillie, C. A., Zafeiropoulos, N., Mwaikambo, L. Y., Ansell, M. P., Dufresne, A., et al. (2001). Current international research into cellulosic fibers and composites. *Journal of Materials Science, 36*, 2107–2131.

Eichhorn, S.J., Gough, J.E., Ulijn, R.V., Sampson, W.W., Kalaskar, D., Cai, S. (2006) Chemical functionalisation and geometrical modification of cellulose fibrous networks for tissue engineering. Abstracts of Papers, 231st ACS National Meeting, Atlanta, GA, United States, March 26–30, 2006, CELL-122.

Favier, V., Canova, G. R., Shrivastava, S. C., & Cavaille, J. Y. (1997). Mechanical percolation in cellulose whisker nanocomposites. *Polymer Engineering and Science, 37*, 1732–1739.

Forster, T. (1948). Intermolecular energy transference and fluorescence. *Ann. Physik [6 Folge], 2*, 55–75.

Furuta, T., & Gray, D. G. (1998). Direct force-distance measurements on wood-pulp fibers in aqueous media. *Journal of Pulp and Paper Science, 24*, 320–324.

Gindl, W., Schoeberl, T., & Keckes, J. (2006). Structure and properties of a pulp fibre-reinforced composite with regenerated cellulose matrix. *Applied Physics A: Materials Science and Processing, 83*, 19–22.

Gordon, G. W., Berry, G., Liang, X. H., Levine, B., & Herman, B. (1998). Quantitative fluorescence resonance energy transfer measurements using fluorescence microscopy. *Biophysical Journal, 74*, 2702–2713.

Goring, D. I. (1965). Thermal softening, adhesive properties and glass transitions in lignin, hemicellulose and cellulose. In *Consolidation of the Paper Web*. *Trans. IIIrd Fund. Res. Symp.* (pp. 555–568). Cambridge: FRC.

Hanley, S. J., & Gray, D. G. (1999). Atomic force microscopy (AFM) images in air and water of kraft pulp fibers. *Journal of Pulp and Paper Science, 25*, 196–200.

Hartler, N., & Mohlin, U.-B. (1975). Cellulose fibre bonding Part 2. Influence of pulping on interfibre bond strength. *Svensk Papperstidning, 78*, 295–299.

Lindstrom, T., Wagberg, L., & Larsson, T. (2005). *On the Nature of Joint Strength in Paper - A Review of Dry and Wet Strength Resins used in Paper Manufacturing 13th FRS*. Cambridge, UK: Pulp and Paper Fundamental Research Society; 2005: pp. 457–562.

McIntosh, D. C., & Leopold, B. (1961). Bonding strength of fibres. In *Formation and Structure of Paper*. *Trans. IInd Fund. Res. Symp* (pp. 265–270). Oxford: FRC.

McKenzie, A. (1984). The structure and properties of paper Part XXI: the diffusion theory of adhesion applied to interfibre bonding. *APPITA, 37*, 580–583.

Mitsui, T., Nakano, H., & Yamana, K. (2000). Coumarin-fluorescein pair as a new donor-acceptor set for fluorescence energy transfer study of DNA. *Tetrahedron Letters, 41*, 2605–2608.

Mohlin, U.-B. (1975). Cellulose fibre bonding Part 4. Effect of chemical modification on rayon fibre bonding ability. *Svensk Papperstidning, 10*, 373–375.

Notley, S. M., Pettersson, B., & Wagberg, L. (2004). Direct measurement of attractive van der Waals' forces between regenerated cellulose surfaces in an aqueous environment. *Journal of the American Chemical Society, 126*, 13930–13931.

Oh, J. K., Tomba, P., Ye, X., Eley, R., Rademacher, J., Farwaha, R., et al. (2003). Film formation and polymer diffusion in poly(vinyl acetate-co-butyl acrylate) latex films. Temperature dependence. *Macromolecules, 36*, 5804–5814.

Pang, L., & Gray, D. G. (1998). Heterogeneous fibrillation of kraft pulp fiber surfaces observed by atomic force microscopy. *Journal of Pulp and Paper Science, 24*, 369–372.

Pekcan, O., Egan, L. S., Winnik, M. A., & Croucher, M. D. (1990). Energy transfer in restricted dimensions: a new approach to latex morphology. *Macromolecules, 23*, 2210–2216.

Pekcan, O., Winnik, M. A., & Croucher, M. D. (1990). Fluorescence studies of coalescence and film formation in poly(methyl methacrylate) nonaqueous dispersion particles. *Macromolecules, 23*, 2673–2678.

Ragauskas, A.J., Williams, C.K., Davison, B.H., Britovsek, G., Cairney, J., Eckert, et al. (2006). The path forward for biofuels and biomaterials. Science (Washington, DC, United States), 311, 484–489.

Somogyi, B., Matko, J., Papp, S., Hevessy, J., Welch, G. R., & Damjanovich, S. (1984). Foerster-type energy transfer as a probe for changes in local fluctuations of the protein matrix. *Biochemistry, 23*, 3403–3411.

Takakusa, H., Kikuchi, K., Urano, Y., Sakamoto, S., Yamaguchi, K., & Nagano, T. (2002). Design and synthesis of an enzyme-cleavable sensor molecule for phosphodiesterase activity based on fluorescence resonance energy transfer. *Journal of the American Chemical Society, 124*, 1653–1657.

Torgnysdotter, A., & Wagberg, L. (2003). Study of the joint strength between regenerated cellulose fibres and its influence on the sheet strength. *Nordic Pulp and Paper Research Journal, 18*, 455–459.

Van Der Meer, B. W., Coker, G., III, & Chen, S. S. Y. (1994). *Resonance energy transfer: Theory and data*. New York: VCH Publishers.

Wong, A. P., & Groves, J. T. (2001). Topographical imaging of an intermembrane junction by combined fluorescence interference and energy transfer microscopies. *Journal of the American Chemical Society, 123*, 12414–12415.

Wong, A. P., & Groves, J. T. (2002). Molecular topography imaging by intermembrane fluorescence resonance energy transfer. *Proceedings of the National Academy of Sciences of the United States of America, 99*, 14147–14152.

Wu, J., Tomba, J. P., Winnik, M. A., Farwaha, R., & Rademacher, J. (2004). Temperature dependence of polymer diffusion in poly(vinyl acetate-co-dibutyl maleate) latex films. *Macromolecules, 37*, 2299–2306.

Zadorecki, P., Karnerfors, H., & Lindenfors, S. (1986). Cellulose fibers as reinforcement in composites: determination of the stiffness of cellulose fibers. *Composites Science and Technology, 27*, 291–303.